

ARTICLE OPEN



Generalizable and transportable resting-state neural signatures characterized by functional networks, neurotransmitters, and clinical symptoms in autism

Takashi Itahashi ^{1,2,1}, Ayumu Yamashita ^{2,3,2,1}, Yuji Takahara^{2,4}, Noriaki Yahata^{2,5,6,7}, Yuta Y. Aoki ^{1,8}, Junya Fujino^{1,9}, Yujiro Yoshihara¹⁰, Motoaki Nakamura¹, Ryuta Aoki^{1,11}, Tsukasa Okimura¹, Haruhisa Ohta¹, Yuki Sakai ^{2,12}, Masahiro Takamura ^{13,14}, Naho Ichikawa ¹³, Go Okada¹³, Naohiro Okada^{6,15}, Kiyoto Kasai ^{6,15,16}, Saori C. Tanaka ^{2,17}, Hiroshi Imamizu ^{2,18}, Nobumasa Kato¹, Yasumasa Okamoto¹³, Hidehiko Takahashi^{9,10,19}, Mitsuo Kawato ^{2,12}, Okito Yamashita^{2,20} and Ryu-ichiro Hashimoto ^{1,2,11}

© The Author(s) 2024

Autism spectrum disorder (ASD) is a lifelong condition with elusive biological mechanisms. The complexity of factors, including inter-site and developmental differences, hinders the development of a generalizable neuroimaging classifier for ASD. Here, we developed a classifier for ASD using a large-scale, multisite resting-state fMRI dataset of 730 Japanese adults, aiming to capture neural signatures that reflect pathophysiology at the functional network level, neurotransmitters, and clinical symptoms of the autistic brain. Our adult ASD classifier was successfully generalized to adults in the United States, Belgium, and Japan. The classifier further demonstrated its successful transportability to children and adolescents. The classifier contained 141 functional connections (FCs) that were important for discriminating individuals with ASD from typically developing controls. These FCs and their terminal brain regions were associated with difficulties in social interaction and dopamine and serotonin, respectively. Finally, we mapped attention-deficit/hyperactivity disorder (ADHD), schizophrenia (SCZ), and major depressive disorder (MDD) onto the biological axis defined by the ASD classifier. ADHD and SCZ, but not MDD, were located proximate to ASD on the biological dimensions. Our results revealed functional signatures of the ASD brain, grounded in molecular characteristics and clinical symptoms, achieving generalizability and transportability applicable to the evaluation of the biological continuity of related diseases.

Molecular Psychiatry; <https://doi.org/10.1038/s41380-024-02759-3>

INTRODUCTION

Establishing robust biomarkers for autism spectrum disorder (ASD) is essential for understanding the pathophysiological mechanisms of this disorder. A plethora of modalities are employed to identify biomarkers for ASD [1]. Yet, no reliable biomarker has been established [2] because of the complicated relationships of various factors, such as genetic and environmental factors [3, 4], biological sex [5], cultural factors [6], and developmental factors [7, 8], all of which form the heterogeneity of ASD. Neuroimaging-based classifiers hold promise in their potential to achieve greater classification accuracy with fewer participants than other approaches, such as genetic biomarkers, which only explain

2.45% of risk variance even with more than 10,000 cases [9, 10]. Nonetheless, several challenges remain in developing robust classifiers.

One critical prerequisite for constructing robust neuroimaging-based classifiers is ensuring their external validity [11]. Despite extensive research dedicated to the development of classifiers for ASD [12–14], 93% of classification studies used the same publicly accessible dataset [15], potentially introducing biases due to repeated use of the same dataset [9, 16]. Some studies have used an inter-site cross-validation scheme to evaluate classifier performance across different imaging sites in the same dataset [17, 18]. However, this approach may not sufficiently evaluate the

¹Medical Institute of Developmental Disabilities Research, Showa University, Tokyo, Japan. ²Brain Information Communication Research Laboratory Group, Advanced Telecommunications Research Institute International, Kyoto, Japan. ³Graduate School of Information Science and Technology, The University of Tokyo, Tokyo, Japan. ⁴Drug Discovery Research Division, Shionogi & Co., Ltd., Osaka, Japan. ⁵Institute for Quantum Life Science, National Institutes for Quantum Science and Technology, Chiba, Japan. ⁶Department of Neuropsychiatry, Graduate School of Medicine, The University of Tokyo, Tokyo, Japan. ⁷Department of Quantum Life Science, Graduate School of Science and Engineering, Chiba University, Chiba, Japan. ⁸Department of Psychiatry, Aoki Clinic, Tokyo, Japan. ⁹Department of Psychiatry and Behavioral Sciences, Graduate School of Medical and Dental Sciences, Tokyo Medical and Dental University, Tokyo, Japan. ¹⁰Department of Psychiatry, Graduate School of Medicine, Kyoto University, Kyoto, Japan. ¹¹Department of Language Sciences, Tokyo Metropolitan University, Tokyo, Japan. ¹²XNef, Inc., Kyoto, Japan. ¹³Department of Psychiatry and Neurosciences, Hiroshima University, Hiroshima, Japan. ¹⁴Department of Neurology, Shimane University, Shimane, Japan. ¹⁵The International Research Center for Neurointelligence (WPI-IRCN) at The University of Tokyo Institutes for Advanced Study (UTIAS), The University of Tokyo, Tokyo, Japan. ¹⁶UTokyo Institute for Diversity and Adaptation of Human Mind (UTIDAHM), The University of Tokyo, Tokyo, Japan. ¹⁷Division of Information Science, Nara Institute of Science and Technology, Nara, Japan. ¹⁸Department of Psychology, Graduate School of Humanities and Sociology, The University of Tokyo, Tokyo, Japan. ¹⁹Center for Brain Integration Research, Tokyo Medical and Dental University, Tokyo, Japan. ²⁰Center for Advanced Intelligence Project, RIKEN, Tokyo, Japan. ²¹These authors contributed equally: Takashi Itahashi, Ayumu Yamashita. email: dbridges50@gmail.com

Received: 10 November 2023 Revised: 10 September 2024 Accepted: 19 September 2024

Published online: 28 September 2024

external validity, because it replicates analyses on the same dataset. Only a few studies have explicitly tested ASD classifiers on entirely independent datasets [9, 19–21]. Another critical challenge in the development of the ASD classifiers is the transportability from one developmental stage to another [22] because the severity of clinical symptoms and patterns of structural and functional alterations in the autistic brain vary with development [23–25]. However, recent large-scale case–control studies on resting-state functional connectivity (FC) have reported the existence of atypical FCs that are reproducible over childhood and adulthood [26, 27]. Because the ASD trait generally persists throughout life, a classifier developed at a particular developmental stage is expected to detect ASD at different developmental stages by capturing development-independent atypical neural signatures.

An often overlooked aspect in classification studies is how well selected features reflect the pathophysiological mechanisms of ASD. Individuals with ASD exhibit alterations in neurotransmitters, including dopamine and serotonin [28–30], and atypical FCs in the autistic brain have been associated with these neurotransmitters [31, 32]. Associating FCs in the ASD classifier with molecular characteristics and clinical symptoms is crucial for understanding the pathophysiological mechanisms underlying ASD. However, previous studies focusing on diagnostic biomarkers have seldom investigated such potential relationships.

Beyond the classification from controls, well-validated classifiers can be used for transdiagnostic investigations into the biological continuum between ASD and other psychiatric disorders. Recently, interest in understanding the biological continuum between ASD and other psychiatric disorders has increased because of overlapping genetic factors and symptoms [33–35]. By treating the classifiers of ASD and other psychiatric disorders as mapping functions, individuals can be projected onto biological axes defined by these classifiers, which enables the investigation of similarities and dissimilarities between categorically distinct disorders in the biological space [19]. Our previous study incorporating the axes defined by classifiers of schizophrenia (SCZ) and ASD revealed that SCZ is more likely to be classified as ASD than typically developing controls (TDCs) on the ASD classifier, whereas ASD is more likely to be classified as TDCs than SCZ on the SCZ classifier [36]. Despite the known high comorbidity of attention-deficit/hyperactivity disorder (ADHD) and major depressive disorder (MDD) with ASD [35, 37], the relationship between ASD and these disorders has not been examined in terms of these biological dimensions. Replicating the relationship with SCZ and exploring the relationships with ADHD and MDD could elucidate the complex relationships between ASD and these disorders.

In this study, we developed a robust classifier for ASD aimed at identifying neural signatures that not only differentiate ASD from TDCs but also reflect the pathophysiological mechanisms underlying ASD. Initially, we constructed an FC-based classifier using the multisite, multi-disease dataset from the Japanese adult population, known as the Strategic Research Program for the Promotion of Brain Science (SRPBS) dataset [38]. This adult ASD classifier was then applied to external validation datasets from the United States, Belgium, and Japan to assess its generalizability across independent imaging sites within the adult population. Furthermore, we evaluated the classifier's transportability to child and adolescent validation datasets to assess whether the adult-based classifier captures the FC alterations present over multiple developmental stages of ASD. After observing that a set of FCs consistently associated with the ASD status have relations with clinical symptoms and neurotransmitter systems, we applied the validated classifiers to examine the relationships between ASD and three major psychiatric disorders, including ADHD, SCZ, and MDD, within a dimensional space defined by the classifiers. Figure 1 presents a detailed overview of our analytical procedures.

MATERIALS AND METHODS

Participants

This study used three adult resting-state functional magnetic resonance imaging (R-fMRI) datasets for the analyses: one was used as the discovery dataset, and the remaining two were used as independent validation datasets to test the generalizability of our classifiers. Furthermore, this study also included three child and adolescent R-fMRI datasets to test the transportability of our classifiers. Data were sourced from three multi-site initiatives: the SRPBS [38], Autism Brain Imaging Data Exchange (ABIDE) [39, 40], Brain/MINDS Beyond (BMB) projects [41], and Healthy Brain Network (HBN) [42]. This study was approved by the institutional review board of Showa University (approval number: B-2014-019), and each local institutional review boards (the Ethics Committee of the Graduate School of Medicine and Faculty of Medicine at the University of Tokyo: 3150; the Ethics Committee of Hiroshima University: E-172 and E-38; and the Committee on Medical Ethics of Kyoto University: C809 and R0027). All the participants and their respective parents/legal guardians provided written informed consent. All procedures were conducted according to the Declaration of Helsinki. Supplementary Method 1 presents the details of the datasets and exclusion criteria. Tables S1, S2, S3 present the demographic information and scanning parameters of the datasets.

R-fMRI data preprocessing and network construction

We preprocessed all the R-fMRI data using fMRIPrep version 1.1.8 [43] and ciftify toolbox version 2.1.1 [44]. Supplementary Method 2 presents the detailed preprocessing steps. We used frame-wise displacement (FD) as a measure for the detection of occasional head movements and removed volumes with $FD > 0.5$ mm, as proposed in a previous study [45]. We used Glasser's 379 surface-based brain parcellations (cortical 360 parcellations and subcortical 19 parcellations) as regions of interest (ROIs) [46]. We computed the temporal correlations of signals among all possible pairs of ROIs and applied Fisher's *t*-to-*z* transformation, resulting in 71,631 unique FCs for each participant. Because the label of each ROI in Glasser's atlas was not intuitive, we used Yeo's resting-state network (RSN) labels to assign important ROIs to the corresponding RSN label [47]. In this study, the subcortical network label was added to the subcortical and cerebellar regions.

A ComBat harmonization method was used to control the imaging site differences that were inherently captured in FCs [48]. In this study, we incorporated disease status (0 = TDC and 1 = ASD), age, and sex as covariates of interest into the ComBat model. Note that we separately applied the ComBat harmonization method to both discovery and independent validation datasets.

Construction of the ASD classifier using the discovery dataset

Based on previous studies [19, 36, 49–52], we assumed that psychiatric disorder factors were associated with a limited number of FCs rather than the whole-brain connections. We used a logistic regression with a least absolute shrinkage and selection operator (LASSO) method [53] that selects an optimal subset of FCs from the whole brain connections. Supplementary Method 3 presents the detailed construction procedures of our ASD classifier. We developed the ASD classifier using the LASSO method with tenfold nested cross-validation (CV) and 10 subsamplings, yielding 100 trained classifiers (Fig. S1). The mean classifier output value was considered as diagnostic probability, which indicates the likelihood of a participant belonging to the ASD class. We considered participants to have the ASD label if their diagnostic probability values were higher than 0.5. We calculated the area under the curve (AUC) to assess the classification performance. Furthermore, the accuracy, sensitivity, specificity, and Matthews correlation coefficient (MCC) were calculated. The MCC is suitable for the imbalanced dataset because this metric considers the ratio of confusion matrix size [54]. We used AUC and MCC as performance indices throughout this paper.

Generalizability of the ASD classifier to the adult validation datasets

We tested the generalizability of the ASD classifier using two independent adult validation datasets: the ABIDE adult and Japanese adult datasets. We applied all the trained classifiers to the independent validation datasets and obtained 100 diagnostic probabilities for each participant. These diagnostic probabilities were averaged for each participant, and a participant was considered to have the ASD label if the mean diagnostic probability was greater than 0.5. To evaluate the classification

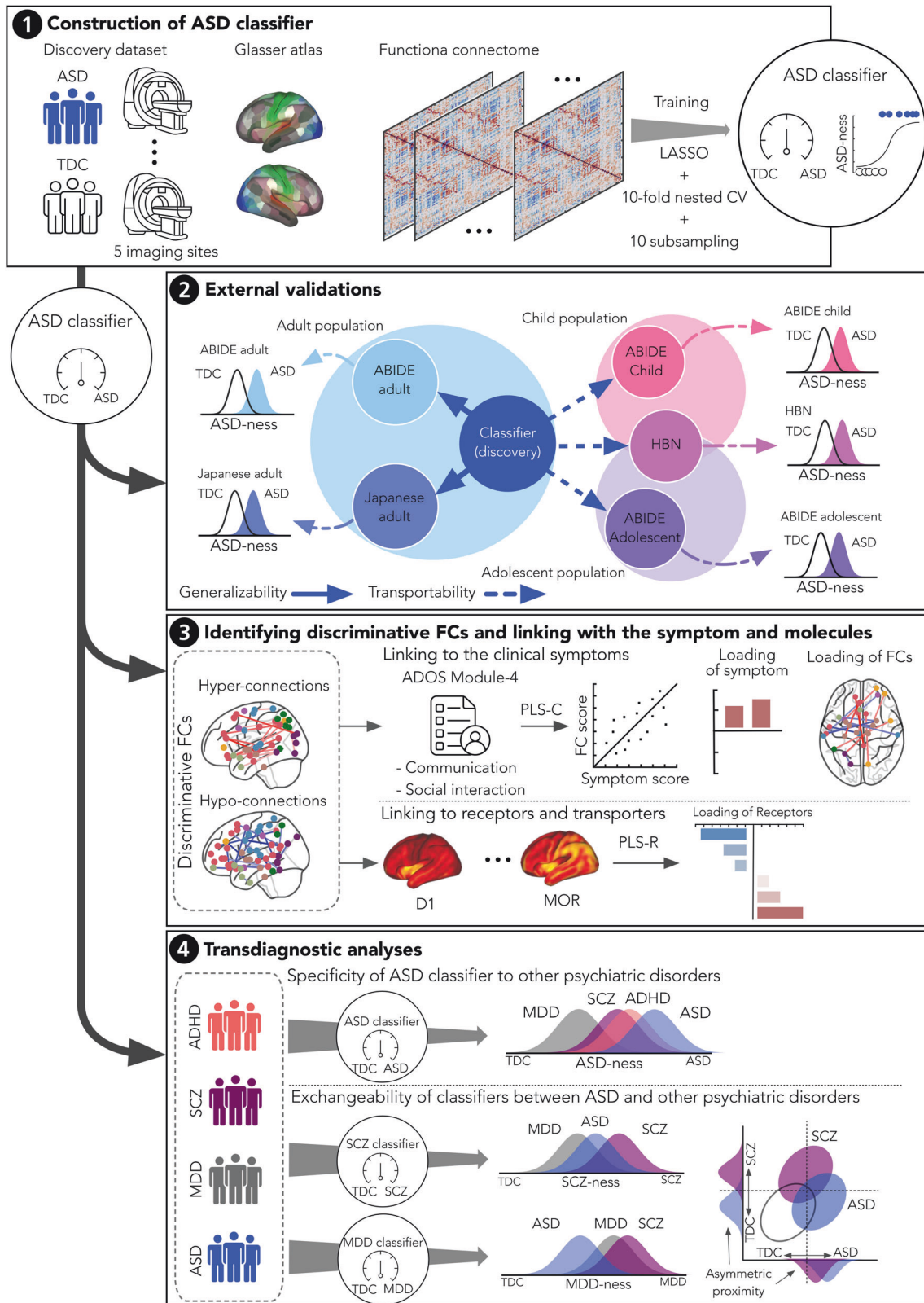


Fig. 1 Overview of analytical procedures. We first constructed a classifier for distinguishing individuals with autism spectrum disorder (ASD) from typically developing controls (TDCs). Glasser's atlas was used to construct a functional connectome for each individual, and a logistic regression with least absolute shrinkage and selection operator (LASSO) was trained using a tenfold nested cross-validation (CV) with 10 subsamples. The external validity (i.e., generalizability and transportability) of the adult ASD classifier was evaluated using five independent validation datasets from different imaging sites and developmental stages. Then, the potential associations of discriminative features with molecular profiles as well as clinical symptoms were evaluated. Finally, the relationships between ASD and other psychiatric disorders were investigated.

performance, the following performance metrics were computed: AUC, accuracy, sensitivity, specificity, and MCC. In this study, we considered that our ASD classifier was generalizable if its classification performance (AUC and MCC) achieved a statistically significant level on the adult validation datasets.

Transportability of the ASD classifier to the child, adolescent, and HBN datasets

We further tested the transportability of the adult ASD classifier to children (age <12 years) and adolescents (12 ≤ age <18 years). We created the child and adolescent datasets using the same exclusion criteria applied to the adult dataset. We further used an additional dataset from the HBN project because this dataset used a unified scanning protocol and mainly contained children and adolescents. Supplementary Method 1 presents the details of the validation datasets to examine transportability. Tables S2, S3 show the demographic information and scanning parameters of the validation datasets. We applied the same preprocessing pipeline and harmonization method to these datasets. In this study, we considered that our ASD classifier was transportable if its classification performance achieved a statistically significant level on the datasets from different developmental stages (i.e., child, adolescent, and HBN).

Evaluation of the statistical significance of the classifier's classification performance

The statistical significance of the AUC and MCC was tested using a permutation test with 500 iterations. At each iteration, we created a permuted dataset by shuffling the diagnostic labels. A classifier was then built for the permuted dataset in the same way as the non-permuted dataset using a tenfold nested CV with 10 subsamples, resulting in 100 permuted classifiers for each iteration. Each individual of the independent datasets was classified based on 100 diagnostic probability values, each of which was generated by 100 trained permuted classifiers. The threshold was set at the mean diagnostic probability value of 0.5. We calculated the AUC and MCC for a permuted classifier in each iteration. We constructed a null distribution for each performance index by aggregating those values across iterations. The statistical threshold was set to 0.05. The Holm–Bonferroni method [55] was used to control the family-wise error (FWE) rate across all validation datasets.

Identifications of FCs associated with the clinical diagnosis of ASD

Discriminative FCs were identified using a permutation test with 500 iterations in a similar manner to our previous study [50]. First, for each FC, we counted the number of times the LASSO selected the FC during the tenfold CV. If a given FC was consistently important for discrimination throughout the training dataset, we expected that it would be selected significantly more times by the LASSO than the chance derived from a null distribution. We shuffled the diagnostic labels at each iteration to create a permuted dataset and constructed permuted classifiers. For each FC, we counted the number of times that the FC was selected by LASSO across tenfold CV and 10 subsamplings (i.e., across 100 classifiers). The maximum counts among all the connections at each iteration were used to construct a null distribution using these maxima. We considered FCs as significant contributors to the ASD status if their *p*-values were below 0.05.

Sensitivity of the ASD classifier to other psychiatric disorders

We tested whether the developed ASD classifier was sensitive to ADHD, SCZ, and MDD. To test this, we applied the classifier to data from ADHD, SCZ, and MDD. The data from SCZ and MDD were included in the SRPBS dataset [38], whereas those from ADHD were collected at Showa University using the same scanning protocol but were not included in the SRPBS dataset. Table S4 presents the details of their demographic information. The same preprocessing pipeline, exclusion criteria, and harmonization method were applied.

We applied 100 trained ASD classifiers to the ADHD, SCZ, and MDD datasets and obtained 100 diagnostic probability values for each participant. We considered a participant to have the ASD label if the mean diagnostic probability was greater than 0.5. We focused on sensitivity rather than other performance indices because the participants with TDC were identical across the datasets. Statistical significance was calculated based on the null distribution obtained from the permutation test with 500 iterations. The statistical threshold was set at $q < 0.05$ after

correcting the false discovery rate (FDR) [56]. The term “proximity” was defined as a condition where other psychiatric disorders exhibited statistically significantly higher sensitivity values than null distribution (i.e., $q < 0.05$) (see Supplementary Method 4 for details).

RESULTS

Testing the generalizability of a Japanese-adult-based classifier for ASD on two adult validation datasets

The classifier built on the discovery dataset (550 adult TDCs and 180 adults with ASD; see Table S1 for participant characteristics) with 71,631 FCs discriminated the ASD group from the TDC group with an accuracy of 76%, AUC of 0.84, and MCC of 0.46. The corresponding sensitivity and specificity were 76 and 75%, respectively (Fig. 2A; see Fig. S2A and Table S5 for the classification performance in each imaging site).

The generalizability of our classifier was tested on the two independent adult validation datasets. For the ABIDE adult dataset, our classifier achieved an accuracy of 62%. The corresponding AUC and MCC were 0.70 and 0.25, respectively (all $p < 0.05$, FWE-corrected). The sensitivity and specificity were 67 and 58%, respectively (Fig. 2B) (see Fig. S2B and Table S5 for the classification performance in each imaging site). These results indicate that our marker has significant discrimination ability in the ABIDE adult dataset. For the newly collected Japanese adult dataset, our classifier exhibited an accuracy of 72% (Fig. 2C and Table S5). The corresponding AUC and MCC were 0.78 and 0.42, respectively (all $p < 0.05$, FWE-corrected). The sensitivity and specificity of this marker were 63 and 78%, respectively. These results suggest that our ASD classifier is generalizable to the adult external validation datasets.

Testing the transportability of the adult ASD classifier on children and adolescents

The transportability of our adult ASD classifier were further tested on the child and adolescent datasets. Our adult ASD classifier exhibited statistically significant classification performance on the children (accuracy = 61%, AUC = 0.66 and MCC = 0.27; $p < 0.05$, FWE-corrected) (Fig. 2D), adolescents (accuracy = 66%, AUC = 0.71, and MCC = 0.32; $p < 0.05$, FWE-corrected) (Fig. 2E), and HBN (accuracy = 62%, AUC = 0.70, and MCC = 0.23; $p < 0.05$, FWE-corrected) (Fig. 2F) datasets. Table S6 shows the classification performance metrics on the external validation datasets. These results suggest that our adult ASD classifier is transportable to other developmental stages, even at independent imaging sites.

Potential factors that affect classification performance

We explored the impacts of head motion, harmonization, and other experimental factors (i.e., diversity in imaging sites and the choice of atlas) on the classification performance. Supplementary Result 1 presents the details. We first assessed whether the head motion artificially improved the generalization performance. A significant positive correlation was not found between the AUC and mean FD ($r = -0.17$, $p = 0.49$; Fig. S3), indicating that head motion did not improve the generalizability of our classifier. Next, the effects of the harmonization method on generalization performance were assessed. In both validation datasets, degraded generalization performance without harmonization was observed (ABIDE adults: accuracy = 60%, AUC = 0.64, and MCC = 0.19; Japanese adults: accuracy = 66%, AUC = 0.75, and MCC = 0.30) (Table S7), supporting the necessity of harmonization methods for improving classification performance. The effects of imaging sites on the generalization performance were then examined because our discovery dataset comprised imaging sites with either an imbalanced patient/control ratio (i.e., COI, KUT, and UTO1) or a different scanning protocol (i.e., UTO2). Neither the inclusion of imbalanced imaging sites nor that of sites with different scanning protocols affected the generalizability of our classifier

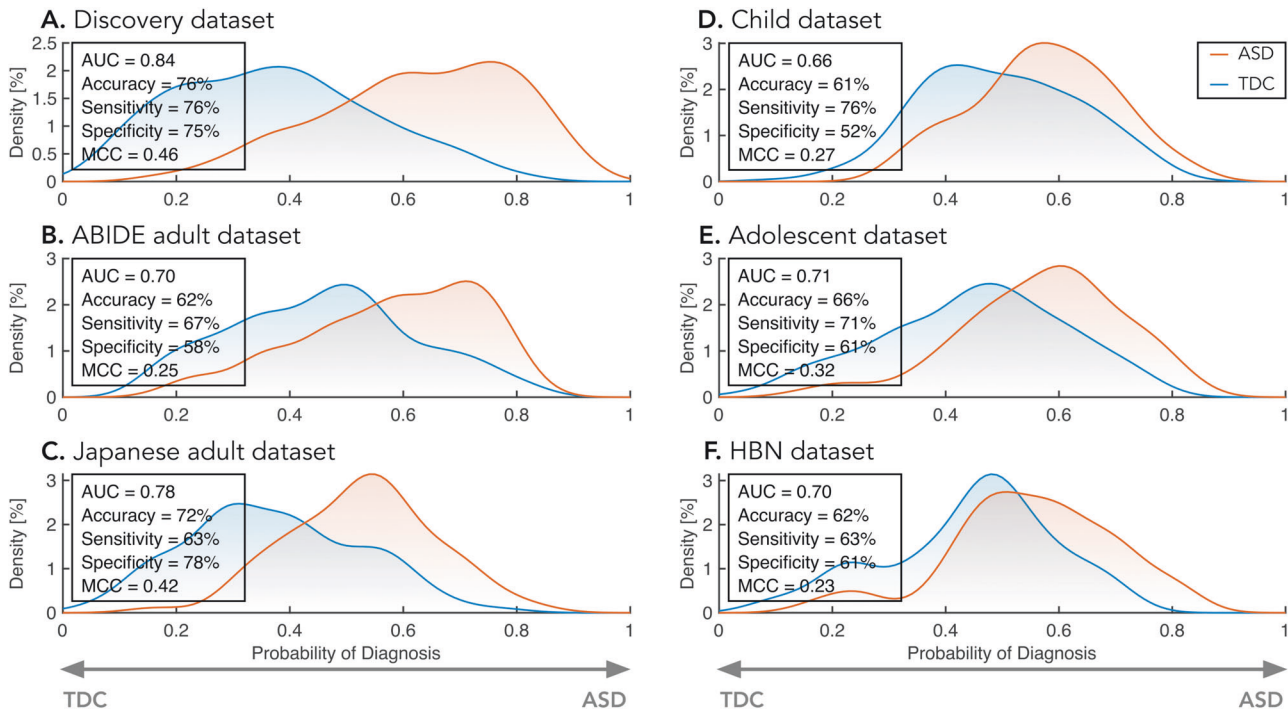


Fig. 2 Classification performance of the ASD classifier in the discovery and five validation datasets. **A** The probability of the ASD diagnosis in the discovery dataset. **B** The probability of the ASD diagnosis in the ABIDE adult validation dataset. **C** The probability of the ASD diagnosis in the Japanese adult validation dataset. **D** The probability of ASD diagnosis in the child dataset. **E** The probability of ASD diagnosis in the adolescent dataset. **F** The probability of ASD diagnosis in the Healthy Brain Network (HBN) dataset. ABIDE Autism Brain Imaging Data Exchange, AUC area under the curve, ASD autism spectrum disorder, MCC Matthews correlation coefficient, and TDC typically developing control.

(Tables S8 and S9). Finally, we checked whether the generalization performance of our ASD classifier was atlas-dependent. We constructed classifiers using the Schaefer cortical atlas [57], which provides atlases with multiple resolution levels ranging from 100 to 900. No improvements specific to the Glasser atlas were observed in the generalization performance (Table S10).

The generalizability and transportability of our ASD classifier on independent validation datasets depended on the assumption that altered FC patterns characteristic of ASD should be reproducible between the discovery and validation datasets. To test this assumption directly, we used a mass-univariate analysis similar to previous studies [50]. The between-group difference for each FC was quantified by calculating the t -value (the diagnosis effect) for each dataset. The Pearson correlation coefficient of the t -values between the datasets was then computed. Statistical significance was tested using a permutation test with 1000 iterations, and the statistical threshold was set at $q < 0.05$ after FDR correction [56]. The discovery dataset showed statistically significant positive correlations with other datasets (ABIDE adult: $r = 0.16$, $q = 0.003$; Japanese adult: $r = 0.35$, $q = 0.000$; adolescent: $r = 0.20$, $q = 0.000$; HBN: $r = 0.08$, $q = 0.044$) except for the child dataset ($r = 0.02$, $q = 0.38$) (Fig. S4).

FCs associated with the ASD diagnosis

A set of discriminative FCs associated with the ASD status was identified (see “Methods” for details): 65 hyper-connections and 76 hypo-connections. These FCs are called “discriminative FCs” hereafter. To examine the spatial distribution of these FCs, we counted the number of occurrences in which each brain region was selected as at least one of the terminations of each discriminative FC. Figure 3A, B shows the spatial distributions of the identified FCs and their terminal regions, respectively. Table S11 provides the connection details. In the cerebral cortex, the bilateral middle and superior temporal gyri (MTG and STG) and

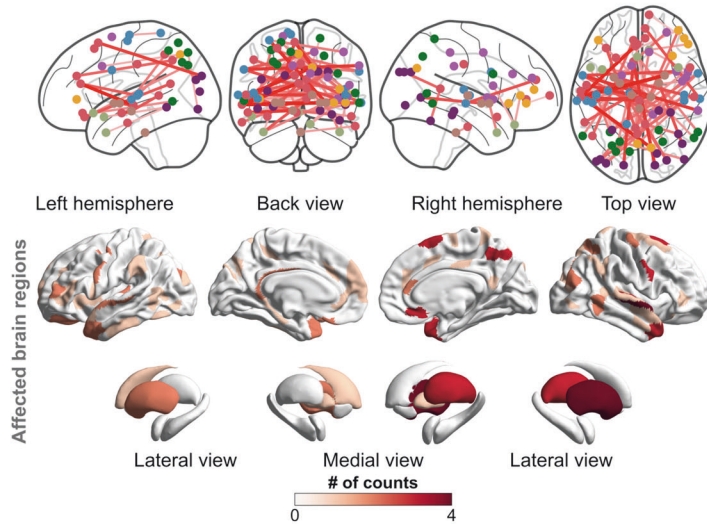
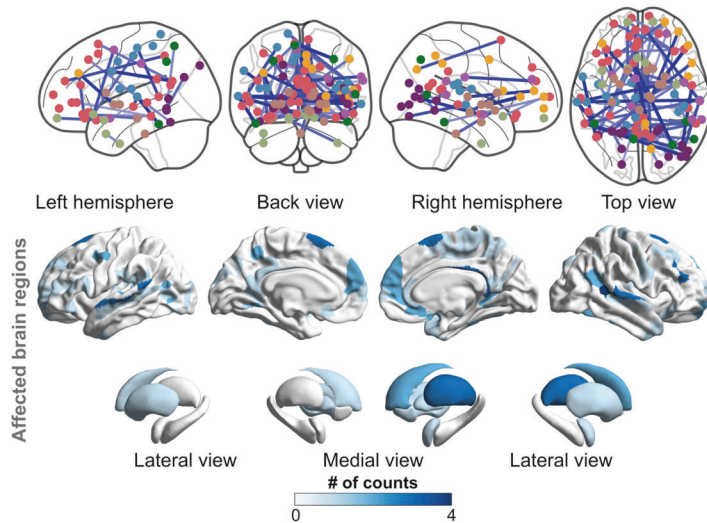
dorsomedial and ventromedial prefrontal cortices (dmPFC and vmPFC) were notably affected. On the other hand, among the subcortical regions, the right thalamus, bilateral putamen, midbrain, and globus pallidus were affected.

To further functionally characterize these FCs, we delineated each of the hyper- and hypo-connections into functional network anatomy (see Supplementary Method 5 for details) [58]. Hyper-connections were dominantly characterized by between-network connections stemming from the subcortical network to other networks, such as the default mode network (DMN) and limbic network (Fig. 3C). On the other hand, hypo-connections were notably characterized by within-network connections of the DMN, limbic, and subcortical networks and between-network connections of the subcortical and frontoparietal networks (FPN) (Fig. 3D).

Linking clinical symptoms and neurotransmitters to discriminative FCs

The association between these discriminative FCs and clinical symptoms was investigated using a partial least squares correlation (PLS-C). The details of the PLS-C procedures are described in Supplementary Method 6. PLS-C identified two latent components (LC1 and LC2) showing statistically significant associations between discriminative FCs and symptoms measured by the Autism Diagnostic Observation Schedule (ADOS) (i.e., Communication [ADOS-A] and Reciprocal Social Interaction [ADOS-B]) (LC1: $r = 0.65$, $q = 0.0024$; LC2: $r = 0.56$, $q = 0.024$ after FDR correction).

For LC1, both ADOS-A and ADOS-B negatively contributed to the symptom-related composite score (ADOS-A: $r = -0.58$, 95% confidence interval [CI] = $[-0.48, -0.68]$, $p < 0.05$; ADOS-B: $r = -0.60$, 95% CI = $[-0.49, -0.69]$, $p < 0.05$). After thresholding the bootstrapped z -scores at ± 1.96 ($p < 0.05$), 17 discriminative FCs were associated with the first FC-related composite score (Fig. 4A and Table S12). Among these 17 FCs, 8 positively

A. Discriminative hyper-connections for the ASD diagnosis**B. Discriminative hypo-connections for the ASD diagnosis**

● DMN ● FPN ● DAN ● VAN ● Limbic ● Somatomotor ● Visual ● Subcortical

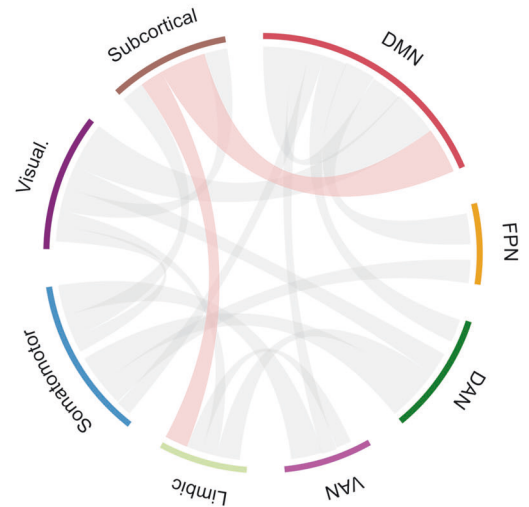
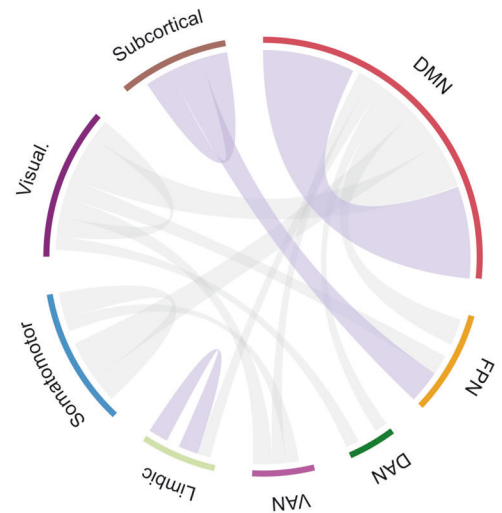
C. Network characterization of hyper-connections**D. Network characterization of hypo-connections**

Fig. 3 Spatial distribution and network-based characterization of discriminative functional connections for the ASD diagnosis. **A** The spatial distribution of discriminative hyper-connections and affected brain regions for the ASD diagnosis. **B** The spatial distribution of discriminative hypo-connections and affected brain regions for the ASD diagnosis. The node color represents the corresponding resting-state network. **C** Network-based characterization of hyper-connections. **D** Network-based characterization of hypo-connections. Edges with red and blue colors indicate that they reach statistical significance ($p < 0.05$ after Bonferroni correction), whereas those with gray color do not. ASD autism spectrum disorder, DAN dorsal attention network, DMN default mode network, FPN frontoparietal network, TDC typically developing control, and VAN ventral attention network.

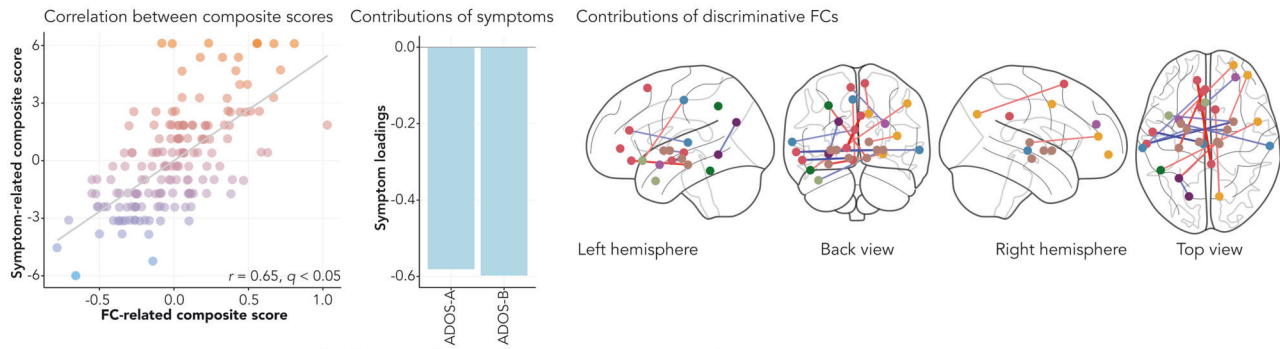
contributed to the FC-related composite score, mainly involving cortico-cortical connections originating from the DMN and FPN to other networks. These eight FCs were negatively correlated with ADOS-A and ADOS-B. The remaining nine FCs negatively contributed to the FC-related composite score, predominantly involving cortico-subcortical connections linking the bilateral putamen and globus pallidus with temporal regions.

For LC2, ADOS-A and ADOS-B exhibited opposite directions of contribution to the symptom-related composite score (ADOS-A: $r = 0.27$, 95% CI = [0.11, 0.42], $p < 0.05$; ADOS-B: $r = -0.26$, 95% CI = [-0.10, -0.42], $p < 0.05$). After thresholding the bootstrapped z-scores, 14 discriminative FCs contributed to the second FC-related composite score (Fig. 4B and Table S12). Six discriminative FCs positively contributed to the FC-related composite score, including cortico-cortical connections originating from the DMN to other

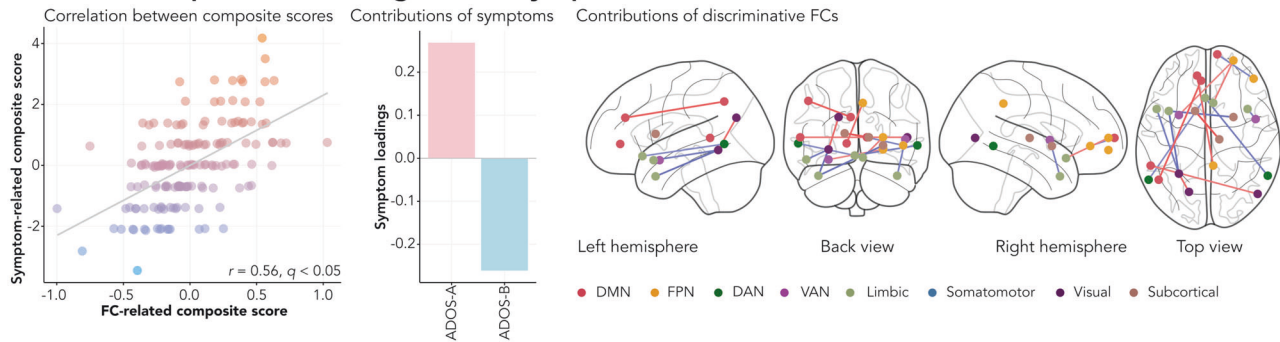
networks. These FCs were positively correlated with ADOS-A while negatively correlated with ADOS-B. The remaining eight FCs negatively contributed to the FC-related composite score, including the connections between the limbic network and other networks. These FCs were negatively correlated with ADOS-A while positively correlated with ADOS-B.

The association between molecular characteristics and terminal brain regions of discriminative FCs was investigated using PLS regression (PLS-R) (see Supplementary Method 7 for details). Population-level molecular templates were estimated using PET tracer studies for 20 receptors and transporters across nine neurotransmitter systems [59, 60], including dopamine, norepinephrine, serotonin, acetylcholine, glutamate, GABA, histamine, cannabinoid, and opioid. The PLS-R identified a statistically significant association between discriminative FCs and receptor/

A. Latent component 1 linking clinical symptoms to discriminative FCs



B. Latent component 2 linking clinical symptoms to discriminative FCs



C. Rank neurotransmitter importance to discriminative FCs

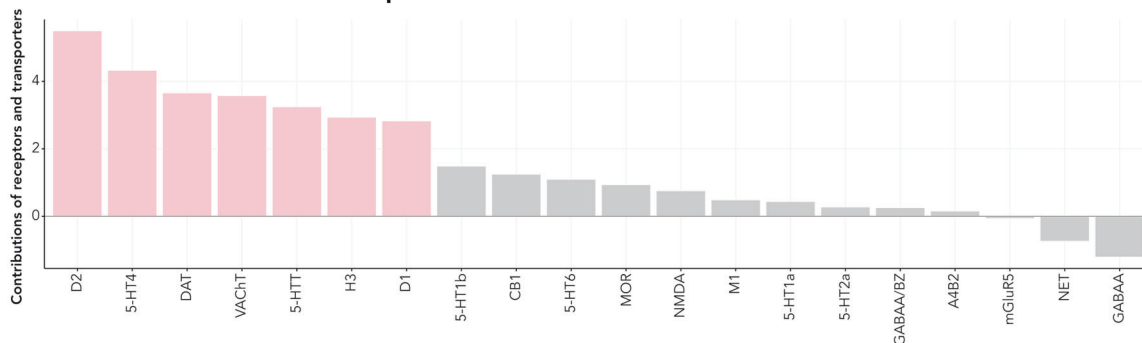


Fig. 4 Associations of the clinical symptoms and neurotransmitters with discriminative FCs. Multivariate statistical methods identified the potential associations of the clinical symptoms and molecular profiles with discriminative FCs. **A** In the first latent component, 17 out of 141 discriminative FCs contributed to the FC-related composite score. FCs in red colors indicate that as the strength of these FCs increases, the severity of both symptoms decreases (i.e., negative correlation), whereas those in blue colors indicate that as the strength of these FCs increases, the severity of symptoms increases (i.e., positive correlation). **B** In the second latent component, FCs with red colors indicate that as the strength of these FCs increases, the severity of ADOS-B decreases (i.e., negative correlation), but the severity of ADOS-A increases (i.e., positive correlation). In contrast, FCs with blue colors indicate that as the strength of these FCs increases, the severity of ADOS-B increases (i.e., positive correlation), but the severity of ADOS-A decreases (i.e., negative correlation). **C** Ranking neurotransmitter importance to discriminative FCs. The pink color indicates statistically significant contributions to discriminative FCs ($p < 0.05$), whereas the gray color indicates statistically insignificant contributions. ADOS Autism Diagnostic Observations Schedule.

transporter densities ($p = 0.001$) and revealed that dopamine (D1, D2, and DAT), serotonin (5-HT4 and 5-HTT), acetylcholine (VACHT), and histamine (H3) significantly contributed to this association ($q < 0.05$) (Fig. 4C).

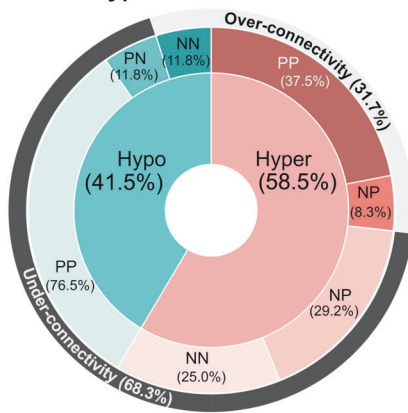
Consistency of discriminative FCs across datasets

Among the 141 discriminative FCs identified by permutation tests, we investigated which discriminative FCs showed consistent alterations across the datasets. We computed a t -value as the effect of diagnosis in each FC of each dataset. Forty-one out of 141 discriminative FCs showed the same sign of t -values across all the datasets (hyper-connection: 59% and hypo-connection: 41%) (Table S13). When considering over- and under-connectivity (i.e., the difference in the absolute values of FC strength between

groups), 68% of the reproducible FCs were under-connectivity (Fig. 5A). The ASD group exhibited atypical connections linking subcortical networks, including the thalamus, putamen, globus pallidus, and midbrain, with other networks, such as the DMN and somatomotor network (Fig. 5B, C).

The statistical significance of the consistency among the six datasets was examined using a binomial test [61]. The number of consistent FCs within the discriminative FCs was 41, whereas the number of FCs showing the same sign of diagnostic effects in the whole FCs (i.e., 71,631 FCs) was 7,083. We assumed a binomial distribution, $Bi(n, p)$, where n stands for the number of discriminative FCs (i.e., $n = 141$), and p stands for the probability of being consistent across the datasets for all FCs (i.e., $p = 7,083/71,631$). The binomial test confirmed that discriminative FCs were

A. Percentages of reproducible hyper- and hypo-connections



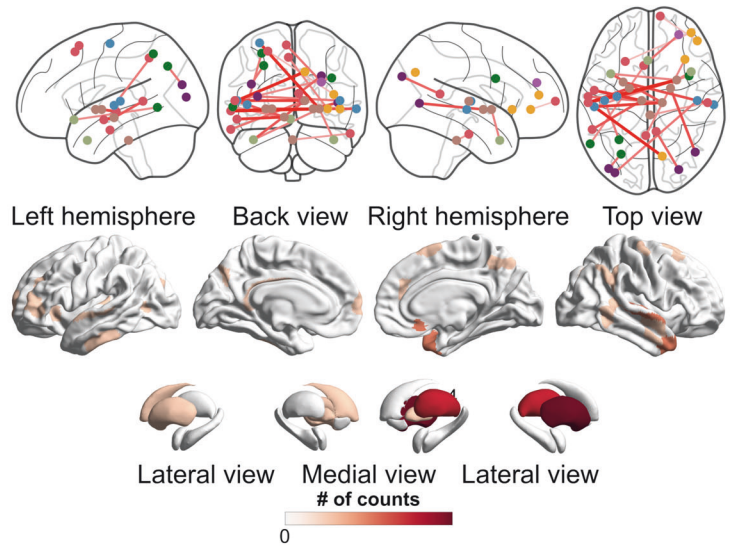
Definitions of subcategories of hyper- and hypo-connections

	TDC	ASD
PP	$r \geq 0$	$r \geq 0$
NP	$r < 0$	$r \geq 0$
PN	$r \geq 0$	$r < 0$
NN	$r < 0$	$r < 0$

Definitions of over- and under-connectivity

Over	$ ASD > TDC $
Under	$ TDC > ASD $

B. Discriminative hyper-connections consistent across cohorts



C. Discriminative hypo-connections consistent across cohorts

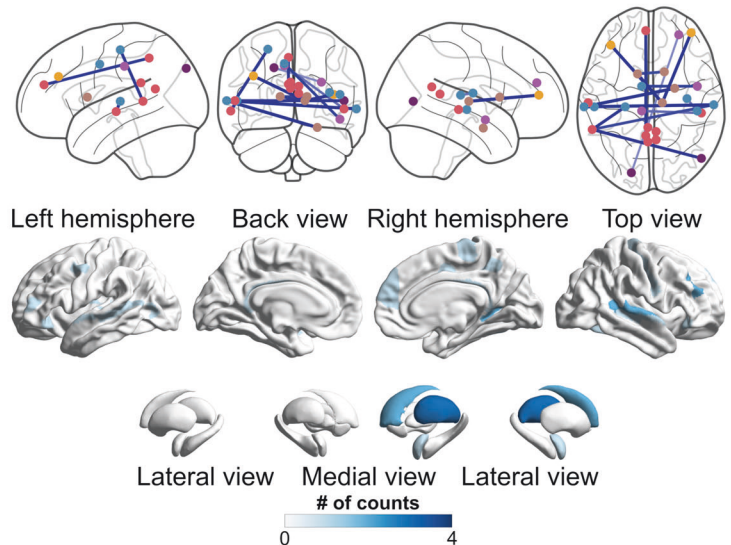


Fig. 5 Distribution of atypical functional connections that are consistent across the datasets. **A** Pie-donut chart showing the details of reproducible hypo- and hyper-connections. **B** The spatial distribution of discriminative hyper-connections consistent across cohorts. **C** The spatial distribution of discriminative hypo-connections consistent across cohorts. DAN dorsal attention network, DMN default mode network, FPN frontoparietal network, L left, N Negative, P positive, R right, and VAN ventral attention network.

reproducible across different ethnicities and cultures (i.e., the United States, Belgium, and Japan) and different developmental stages (i.e., children, adolescents, and adults) ($q < 0.05$). The binomial tests confirmed the statistical significance of the consistency between the discovery dataset and every dataset (see Supplementary Result 2 for details). These results indicate that our ASD classifier selects FCs that show consistent alterations across independent imaging sites and developmental stages, which may yield acceptable classification performance in the independent validation datasets.

Sensitivity of the ASD classifier to other psychiatric disorders

Our ASD classifier was applied to ADHD, SCZ, and MDD to test its specificity. Our ASD classifier exhibited sensitivities of 58%, 56%, and 33% for ADHD, SCZ, and MDD, respectively (Fig. 6A). As expected, the sensitivities for the three disorders were lower than that for the ASD diagnosis. However, the sensitivities to the ADHD

and SCZ diagnoses remained statistically significant (ADHD: $q = 0.018$ and SCZ: $q = 0.021$), whereas the classifier showed no sensitivity to the MDD diagnosis ($q = 0.638$). These results indicate that ADHD and SCZ, but not MDD, were located proximate to ASD on the biological dimension defined by the ASD classifier.

Relationships between ASD and other psychiatric disorders on biological dimensions defined by classifiers

To further explore the relationships between ASD and other psychiatric disorders on multiple biological axes, two additional classifiers for the SCZ and MDD were developed (see Table S14 for the classification performance of both classifiers). No classifier for the ADHD group was developed due to the limited number of participants with ADHD ($n = 62$). After constructing the SCZ and MDD classifiers, each classifier was applied to ASD (see Supplementary Method 8). The details and results examining the relationship among other psychiatric disorders are described in

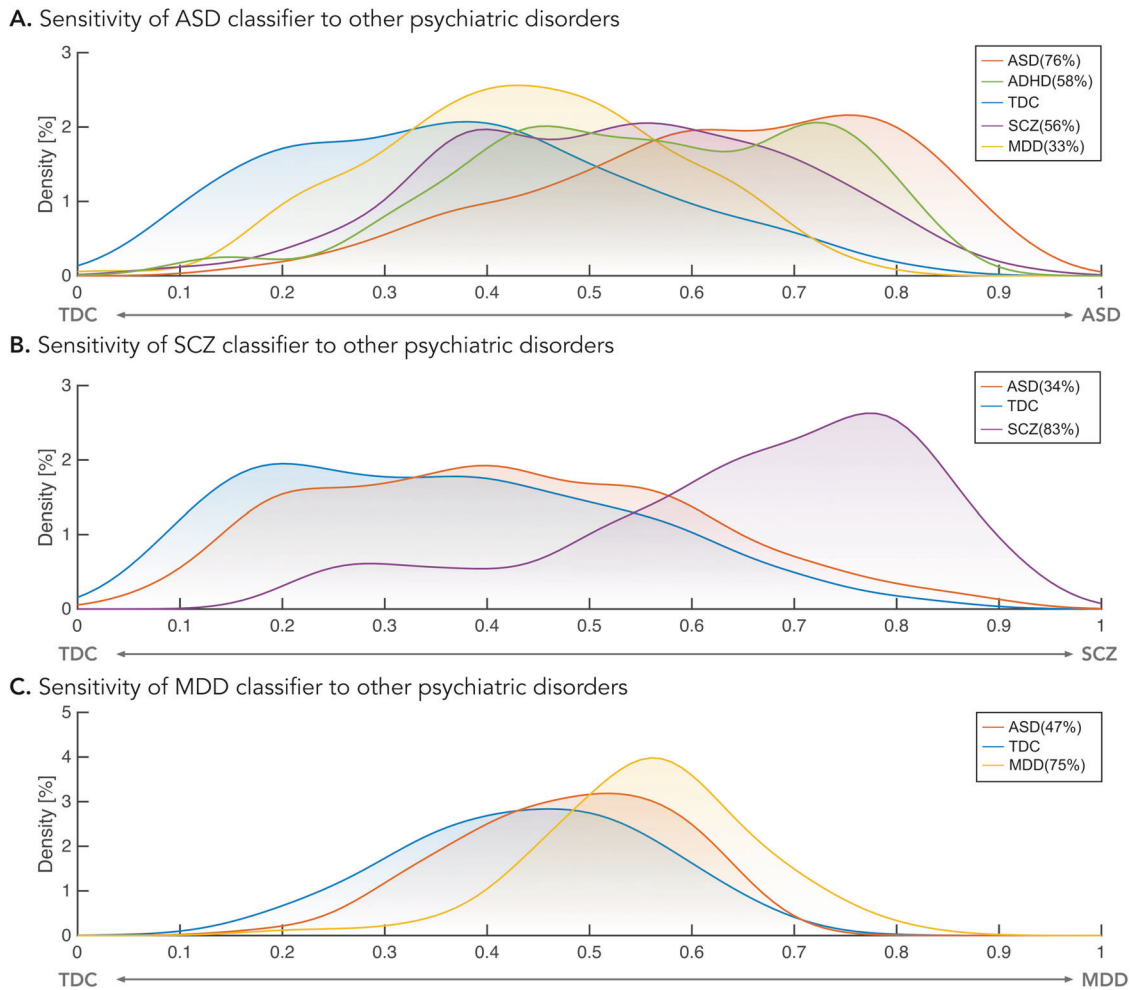


Fig. 6 Relationships between ASD and other psychiatric disorders on the biological axes defined by each classifier. A Sensitivity of the classifier for autism spectrum disorder (ASD) to attention-deficit/hyperactivity disorder (ADHD), schizophrenia (SCZ), and major depressive disorder (MDD). **B** Sensitivity of the SCZ classifier to ASD. **C** Sensitivity of the MDD classifier to ASD.

Supplementary Result 3. The SCZ classifier exhibited poor sensitivity to the ASD diagnosis (34%) (Fig. 6B), supporting the view of the asymmetric proximity between ASD and SCZ [36]. On the other hand, the MDD classifier showed poor sensitivity to the ASD diagnosis (47%) (Fig. 6C), indicating no proximate relationship on the defined axes between ASD and MDD. These results suggest that ASD is not located proximate to SCZ and MDD on the biological axes defined by the SCZ and MDD classifiers. Further evidence is provided in Supplementary Result 4.

DISCUSSION

In this study, we developed an FC-based ASD classifier using the Japanese adult multi-site dataset. Our ASD classifier was generalizable to the ABIDE and Japanese adults from independent imaging sites with an AUC value of >70%. Furthermore, this classifier demonstrated acceptable classification performance in children and adolescents (i.e., child, adolescent, and HBN datasets), indicating the presence of an atypical neural basis that persists in ASD from childhood to adulthood. We identified 141 FCs pivotal for determining ASD status, spanning multiple networks, including the DMN, limbic, FPN, and subcortical networks. These FCs comprised social brain regions, such as the vmPFC, dmPFC, STG, midbrain, and thalamus, and were associated with difficulties in social communication and neurotransmitters. Notably, 41 out of 141 FCs displayed consistent diagnostic effects

across all six datasets. By using our classifier as a biological axis and mapping ADHD, SCZ, and MDD onto this axis, we observed proximity between ASD and ADHD as well as SCZ, with a greater distance between ASD and MDD. These findings provide novel insights into the neural underpinnings of the autistic brain and offer an effective tool for elucidating transdiagnostic continuity.

In this study, the robustness of our classifier was confirmed through stringent evaluations of its generalizability and transportability on independent validation datasets. Most prior studies have relied on CV procedures in the ABIDE dataset [14, 15], which may overestimate classification performance and introduce biases [9, 16]. Therefore, evaluation of the generalization performance of a classifier using completely independent external datasets is crucial [62]. A few studies have evaluated the generalizability of their classifiers using independent validation datasets, and they have reported generalization performance ranging from 67 to 75% [9, 19, 20], which is comparable to our results. Our study's strength lies in the thorough evaluation of generalization performance. The generalizability and transportability of our classifier were verified using five independent validation datasets that differed in imaging sites, ethnic and cultural backgrounds, and developmental stages. Furthermore, we confirmed that our the generalizability of our classifier remained intact when using another brain atlas featuring multiple resolution levels (Table S10). These evaluations ensure the robustness of our classifier and provide a new tool to explore hypotheses in the autistic brain.

Development-dependent changes in FCs hinder the transfer of classifiers to other developmental stages [63, 64]. Nevertheless, our adult ASD classifier successfully distinguished children and adolescents with ASD from TDCs. The transportability of our adult ASD classifier may be due to the LASSO method used in this study. The autistic brain likely presents a mosaic pattern of age-specific and age-unspecific atypical FCs [65–67]. Supporting this view, Alaerts and colleagues reported that, depending on the terminal regions, the posterior superior temporal sulcus exhibits distinct age-related patterns of abnormal FCs in the autistic brain [24]. In such a complicated situation, non-sparse machine learning algorithms like support vector machines may fail to select features appropriately, thereby yielding reduced generalization performance when transferring classifiers to other developmental stages. The LASSO method tends to choose atypical FCs consistent within the discovery dataset during nested CV, resulting in the selection of dataset-independent atypical FCs in our adult ASD classifier.

Our ASD classifier identified 141 discriminative FCs distributed across multiple networks, particularly the DMN and subcortical networks. A prominent feature of these discriminative FCs is their association with clinical symptoms and corresponding terminal brain regions associated with molecular profiles. Consistent with prior findings [26, 67–69], FCs within and between the DMN and subcortical networks are predominantly associated with challenges in communication and reciprocal social interaction. Furthermore, the terminal brain regions of these discriminative FCs are dominantly associated with dopamine and serotonin, which have been recurrently implicated in ASD [31, 70, 71]. Therefore, these discriminative FCs may reflect the pathophysiological mechanisms underlying the autistic brain.

Another notable feature is the alterations in FCs within and between subcortical, DMN, and somatomotor networks, involving regions such as the thalamus, putamen, globus pallidus, midbrain, and STG. Of the 41 discriminative FCs that exhibited consistent ASD status effects across the six datasets, 38 involved terminal brain regions within these networks. Our findings suggest that abnormalities in these networks serve as the core neural basis for this disorder. Supporting this possibility, several lines of evidence indicate functional alterations within and between the subcortical, DMN, and somatomotor networks [66–69] and their associations with clinical symptoms, such as restricted and repetitive behaviors and atypical sensory processing [26, 58]. Furthermore, the association between atypical sensory processing and socio-communicative impairments is supported by previous studies [72, 73]. The replication, associations with core symptoms, and consistency of abnormalities across developmental stages may distinguish these networks as the core basis for ASD.

We demonstrated the applicability of our classifier-based analytic framework to examine the biological continuum of ASD with ADHD, SCZ, and MDD by mapping these disorders onto the biological dimensions defined by the classifiers. ASD and ADHD have a marked overlap in underlying genetic and environmental influences [35]. On the biological axis delineated by our ASD classifier, ADHD was positioned close to ASD, suggesting a potential partial overlap between the two conditions. On the other hand, the comorbidity rate of MDD in ASD is as high as 11% [37]. However, MDD was not situated near ASD on this axis, indicating that ASD and MDD involve distinct neural circuits even though symptoms may partially overlap. Previous studies have highlighted the substantial overlap between ASD and SCZ at genetic [74], neural [75], and behavioral levels [76], although these findings are less replicable because of methodological differences [77]. In contrast, our approach for mapping individuals into the biological space defined by the resting-state FC classifier reproduced the asymmetric proximity between the ASD and SCZ groups. In particular, the SCZ group showed stronger adjacency to the ASD group than the TDC group on the ASD

classifier, while the ASD group displayed stronger proximity to the TDC group than the SCZ group on the SCZ classifier. This was observed, using different datasets and methods [36]. Our replicable approach may provide clues for investigating spectrum structures in psychiatric disorders.

Recent trends in autism research have increasingly shifted from viewing ASD as a single entity to recognizing it as a broad spectrum comprising distinct subtypes [32, 78–80] or idiosyncrasies [81–83]. Consequently, one may be skeptical about approaches like ours that treat ASD as a homogeneous group and develop markers for its label. However, our approach does not contradict such dominant views. While ASD presents varying patterns and degrees of symptoms that meet diagnostic criteria, we posit that there are underlying biological commonalities, albeit to varying degrees. If these commonalities do not exist, classifiers will fail to accurately predict diagnostic labels. However, our results did not support this expectation. The identification of shared neural signatures could facilitate the stratification and personalized treatment of ASD. Furthermore, in neuroimaging-based stratification, the high dimensionality of features and the inclusion of irrelevant features may impede the identification of reproducible subtypes that reflect pathological mechanisms [84]. Our ASD classifier, employing LASSO, prunes irrelevant FCs and selects 141 discriminative FCs from 71,631 FCs. The collection of neural signatures associated with ASD diagnosis may reflect, to varying degrees, the pathological mechanisms of ASD and could serve as an effective feature reduction method for the stratifying of ASD. Moreover, identifying these neural signatures allows for the assessment of co-fluctuations between symptoms and neural signatures at the individual level, potentially enabling tailored interventions such as repetitive transcranial magnetic stimulation and neurofeedback [85].

The current study has several limitations. First, we did not examine the generalizability of our classifier to individuals with ASD who also exhibit intellectual disability (i.e., full-scale IQ \leq 70). According to the Centers for Disease Control and Prevention, 31% of individuals with ASD have intellectual disability, whereas 23% of those with ASD fall within the borderline range (i.e., 70 < full-scale IQ \leq 85) [86]. Thus, our datasets may not fully represent the characteristics of the ASD population. A recent study, however, has demonstrated that individuals with ASD who have low full-scale IQ scores exhibit hypo-connections within the DMN [87], which is consistent with our findings. Second, although our ASD classifier demonstrated statistically significant classification performance across all six datasets, a reduction in performance was observed for the ABIDE and HBN datasets. Detailed investigations suggest that factors such as ethnic diversity among the datasets influence this decline (see Supplementary Result 5 for details). Future studies incorporating participants with ethnically diverse backgrounds may be essential for constructing generalizable neuroimaging-based markers of ASD. Finally, the correlative nature of the current design does not allow us to reveal causal relationships between identified FCs and the etiology of ASD. However, the LASSO method was used to increase the interpretability of important FCs and mitigate over-fitting [88]. Our findings pave the way for future research to explore possible causal relationships by combining the identified FCs with neuromodulation techniques.

In conclusion, we developed an adult ASD classifier that is generalizable and transportable to diverse validation datasets from independent imaging sites and across different developmental stages. The identified FCs were largely delineated within and between the DMN, subcortical, and somatomotor networks, which is consistent with previous evidence. These FCs were found to be associated with social communication difficulties, and their terminal brain regions were dominantly associated with dopamine and serotonin. Furthermore, we demonstrated the utility of our classifier to examine the effects of developmental stages on the

autistic brain and the biological continuum between ASD and other psychiatric disorders. Using discriminative FCs identified by our ASD classifier, prospective future directions will be opened, including identifying biological subtypes within ASD and interventions based on these FCs as targets.

DATA AVAILABILITY

All discovery data, except for a part of the discovery dataset (i.e., SWA1 and UTO2), are available from the Decoded Neurofeedback (DecNef) Project Brain Data Repository (<https://bicr-resource.atr.jp/decnefpro/>). ABIDE-I and ABIDE-II are available from https://fcon_1000.projects.nitrc.org/indi/abide/. The BMB data will be available from its project website (<https://hbm.brainminds-beyond.jp/>). The HBN data are available from https://fcon_1000.projects.nitrc.org/indi/cmi_healthy_brain_network/.

CODE AVAILABILITY

All the codes used in this study can be obtained from the corresponding author upon request.

REFERENCES

- Parellada M, Andreu-Bernabeu Á, Burdeus M, San José Cáceres A, Urbiola E, Carpenter LL, et al. In search of biomarkers to guide interventions in autism spectrum disorder: a systematic review. *Am J Psychiatry*. 2023;180:23–40.
- Cortese S, Solmi M, Michelini G, Bellato A, Blanner C, Canozzi A, et al. Candidate diagnostic biomarkers for neurodevelopmental disorders in children and adolescents: a systematic review. *World Psychiatry*. 2023;22:129–49.
- Hallmayer J, Cleveland S, Torres A, Phillips J, Cohen B, Torigoe T, et al. Genetic heritability and shared environmental factors among twin pairs with autism. *Arch Gen Psychiatry*. 2011;68:1095–102.
- Colvert E, Tick B, McEwen F, Stewart C, Curran SR, Woodhouse E, et al. Heritability of autism spectrum disorder in a UK population-based twin sample. *JAMA Psychiatry*. 2015;72:415–23.
- Floris DL, Peng H, Warrier V, Lombardo MV, Pretzsch CM, Moreau C, et al. The link between autism and sex-related neuroanatomy, and associated cognition and gene expression. *Am J Psychiatry*. 2022;180:50–64. [appi.ajp.2022.180.050](https://doi.org/10.1176/appi.ajp.2022.180.050)
- de Leeuw A, Happé F, Hoekstra RA. A conceptual framework for understanding the cultural and contextual factors on autism across the globe. *Autism Res*. 2020;13:1029–50.
- Fountain C, Winter AS, Bearman PS. Six developmental trajectories characterize children with autism. *Pediatrics*. 2012;129:e1112–e1120.
- Waizbard-Bartov E, Ferrer E, Heath B, Rogers SJ, Nordahl CW, Solomon M, et al. Identifying autism symptom severity trajectories across childhood. *Autism Res*. 2022;15:687–701.
- Traut N, Heuer K, Lemaître G, Beggiano A, Germanaud D, Elmaleh M, et al. Insights from an autism imaging biomarker challenge: Promises and threats to biomarker discovery. *Neuroimage*. 2022;255:119171.
- Grove J, Ripke S, Als TD, Mattheisen M, Walters RK, Won H, et al. Identification of common genetic risk variants for autism spectrum disorder. *Nat Genet*. 2019;51:431–44.
- Ho SY, Phua K, Wong L, Bin Goh WW. Extensions of the external validation for checking learned model interpretability and generalizability. *Patterns (N Y)*. 2020;1:100129.
- Feng W, Liu G, Zeng K, Zeng M, Liu Y. A review of methods for classification and recognition of ASD using fMRI data. *J Neurosci Methods*. 2021;368:109456.
- Horien C, Floris DL, Greene AS, Noble S, Rolison M, Tejavibulya L, et al. Functional connectome-based predictive modeling in autism. *Biol Psychiatry*. 2022;92:626–42.
- Wolfers T, Floris DL, Dinga R, van Rooij D, Isakoglou C, Kia SM, et al. From pattern classification to stratification: towards conceptualizing the heterogeneity of Autism Spectrum Disorder. *Neurosci Biobehav Rev*. 2019;104:240–54.
- Santana CP, de Carvalho EA, Rodrigues ID, Bastos GS, de Souza AD, de Brito LL. rs-fMRI and machine learning for ASD diagnosis: a systematic review and meta-analysis. *Sci Rep*. 2022;12:6030.
- Thompson WH, Wright J, Bissett PG, Poldrack RA. Dataset decay and the problem of sequential analyses on open datasets. *Elife*. 2020;9:e53498.
- Spera G, Retico A, Bosco P, Ferrari E, Palumbo L, Oliva P, et al. Evaluation of altered functional connections in male children with autism spectrum disorders on multiple-site data optimized with machine learning. *Front Psychiatry*. 2019;10:620.
- Abraham A, Milham MP, Di Martino A, Craddock RC, Samaras D, Thirion B, et al. Deriving reproducible biomarkers from multi-site resting-state data: An Autism-based example. *Neuroimage*. 2017;147:736–45.
- Yahata N, Morimoto J, Hashimoto R, Lisi G, Shibata K, Kawakubo Y, et al. A small number of abnormal brain connections predicts adult autism spectrum disorder. *Nat Commun*. 2016;7:11254.
- Jahedi A, Nasamran CA, Faires B, Fan J, Müller R-A. Distributed intrinsic functional connectivity patterns predict diagnostic status in large autism cohort. *Brain Connect*. 2017;7:515–25.
- Supekar K, Ryali S, Yuan R, Kumar D, de los Angeles C, Menon V. Robust, generalizable, and interpretable artificial intelligence-derived brain fingerprints of autism and social communication symptom severity. *Biol Psychiatry*. 2022;92:643–53.
- Degtiar I, Rose S. A review of generalizability and transportability. *Ann Rev Stat Appl*. 2023;10:501–24.
- Uddin LQ, Supekar K, Menon V. Reconceptualizing functional brain connectivity in autism from a developmental perspective. *Front Hum Neurosci*. 2013;7:458.
- Alaerts K, Nayar K, Kelly C, Raithel J, Milham MP, Di Martino A. Age-related changes in intrinsic function of the superior temporal sulcus in autism spectrum disorders. *Soc Cogn Affect Neurosci*. 2015;10:1413–23.
- Wallace GL, Dankner N, Kenworthy L, Giedd JN, Martin A. Age-related temporal and parietal cortical thinning in autism spectrum disorders. *Brain*. 2010;133:3745–54.
- Ilioska I, Oldehinkel M, Llera A, Chopra S, Looden T, Chauvin R, et al. Connectome-wide mega-analysis reveals robust patterns of atypical functional connectivity in autism. *Biol Psychiatry*. 2023;94:29–39.
- Holiga Š, Hipp JF, Chatham CH, Garces P, Spooren W, D’Ardhuy XL, et al. Patients with autism spectrum disorders display reproducible functional connectivity alterations. *Sci Transl Med*. 2019;11:eaat9223.
- Nakamura K, Sekine Y, Ouchi Y, Tsujii M, Yoshikawa E, Futatsubashi M, et al. Brain serotonin and dopamine transporter bindings in adults with high-functioning autism. *Arch Gen Psychiatry*. 2010;67:59–68.
- Garbarino VR, Gilman TL, Daws LC, Gould GG. Extreme enhancement or depletion of serotonin transporter function and serotonin availability in autism spectrum disorder. *Pharmacol Res*. 2019;140:85–99.
- Jaiswal P, Mohanakumar KP, Rajamma U. Serotonin mediated immunoregulation and neural functions: Complicity in the aetiology of autism spectrum disorders. *Neurosci Biobehav Rev*. 2015;55:413–31.
- Murayama C, Iwabuchi T, Kato Y, Yokokura M, Harada T, Goto T, et al. Extrastriatal dopamine D2/3 receptor binding, functional connectivity, and autism socio-communicational deficits: a PET and fMRI study. *Mol Psychiatry*. 2022;27:2106–13.
- Buch AM, Vértes PE, Seidlitz J, Kim SH, Grosenick L, Liston C. Molecular and network-level mechanisms explaining individual differences in autism spectrum disorder. *Nat Neurosci*. 2023;26:650–63. 1–14
- Aoki Y, Yoncheva YN, Chen B, Nath T, Sharp D, Lazar M, et al. Association of white matter structure with autism spectrum disorder and attention-deficit/hyperactivity disorder. *JAMA Psychiatry*. 2017;74:1120–8.
- Ardesch DJ, Libedinsky I, Scholtens LH, Wei Y, van den Heuvel MP. Convergence of brain transcriptomic and neuroimaging patterns in schizophrenia, bipolar disorder, autism spectrum disorder, and major depressive disorder. *Biol Psychiatry Cogn Neurosci Neuroimaging*. 2023;8:630–9.
- Thapar A, Cooper M, Rutter M. Neurodevelopmental disorders. *Lancet Psychiatry*. 2017;4:339–46.
- Yoshihara Y, Lisi G, Yahata N, Fujino J, Matsumoto Y, Miyata J, et al. Overlapping but asymmetrical relationships between schizophrenia and autism revealed by brain connectivity. *Schizophr Bull*. 2020. <https://doi.org/10.1093/schbul/sbaa021>.
- Lai M-C, Kasseh C, Besney R, Bonato S, Hull L, Mandy W, et al. Prevalence of co-occurring mental health diagnoses in the autism population: a systematic review and meta-analysis. *Lancet Psychiatry*. 2019;6:819–29.
- Tanaka SC, Yamashita A, Yahata N, Itahashi T, Lisi G, Yamada T, et al. A multi-site, multi-disorder resting-state magnetic resonance image database. *Sci Data*. 2021;8:227.
- Di Martino A, Yan C-G, Li Q, Denio E, Castellanos FX, Alaerts K, et al. The autism brain imaging data exchange: towards a large-scale evaluation of the intrinsic brain architecture in autism. *Mol Psychiatry*. 2014;19:659–67.
- Di Martino A, O’Connor D, Chen B, Alaerts K, Anderson JS, Assaf M, et al. Enhancing studies of the connectome in autism using the autism brain imaging data exchange II. *Sci Data*. 2017;4:170010.
- Koike S, Tanaka SC, Okada T, Aso T, Yamashita A, Yamashita O, et al. Brain/MINDS beyond human brain MRI project: a protocol for multi-level harmonization across brain disorders throughout the lifespan. *Neuroimage Clin*. 2021;30:102600.
- Alexander LM, Escalera J, Ai L, Andreotti C, Febre K, Mangone A, et al. An open resource for transdiagnostic research in pediatric mental health and learning disorders. *Sci Data*. 2017;4:170181.
- Esteban O, Markiewicz CJ, Blair RW, Moodie CA, Isik AI, Erramuzpe A, et al. fMRIPrep: a robust preprocessing pipeline for functional MRI. *Nat Methods*. 2019;16:111–6.
- Dickie EW, Anticevic A, Smith DE, Coalson TS, Manogaran M, Calarco N, et al. Cifity: a framework for surface-based analysis of legacy MR acquisitions. *Neuroimage*. 2019;197:818–26.

45. Power JD, Barnes KA, Snyder AZ, Schlaggar BL, Petersen SE. Spurious but systematic correlations in functional connectivity MRI networks arise from subject motion. *Neuroimage*. 2012;59:2142–54.
46. Glasser MF, Coalson TS, Robinson EC, Hacker CD, Harwell J, Yacoub E, et al. A multi-modal parcellation of human cerebral cortex. *Nature*. 2016;536:171–8.
47. Yeo BTT, Krienen FM, Sepulcre J, Sabuncu MR, Lashkari D, Hollinshead M, et al. The organization of the human cerebral cortex estimated by intrinsic functional connectivity. *J Neurophysiol*. 2011;106:1125–65.
48. Johnson WE, Li C, Rabinovic A. Adjusting batch effects in microarray expression data using empirical Bayes methods. *Biostatistics*. 2007;8:118–27.
49. Ichikawa N, Lisi G, Yahata N, Okada G, Takamura M, Hashimoto R-I, et al. Primary functional brain connections associated with melancholic major depressive disorder and modulation by antidepressants. *Sci Rep*. 2020;10:3542.
50. Yamashita A, Sakai Y, Yamada T, Yahata N, Kunimatsu A, Okada N, et al. Generalizable brain network markers of major depressive disorder across multiple imaging sites. *PLoS Biol*. 2020;18:e3000966.
51. Almuqhim F, Saeed F. ASD-SANet: a sparse autoencoder, and deep-neural network model for detecting autism spectrum disorder (ASD) using fMRI data. *Front Comput Neurosci*. 2021;15:654315.
52. Kwon H, Kim JI, Son S-Y, Jang YH, Kim B-N, Lee HJ, et al. Sparse Hierarchical Representation Learning on Functional Brain Networks for Prediction of Autism Severity Levels. *Front Neurosci*. 2022;16:935431.
53. Tibshirani R. Regression shrinkage and selection via the lasso. *J R Stat Soc*. 1996;58:267–88.
54. Chicco D. Ten quick tips for machine learning in computational biology. *BioData Min*. 2017;10:35.
55. Holm S. A simple sequentially rejective multiple test procedure. *Scand Stat Theory Appl*. 1979;6:65–70.
56. Benjamini Y, Hochberg Y. Controlling the false discovery rate: a practical and powerful approach to multiple testing. *J R Stat Soc*. 1995;57:289–300.
57. Schaefer A, Kong R, Gordon EM, Laumann TO, Zuo X-N, Holmes AJ, et al. Local-global parcellation of the human cerebral cortex from intrinsic functional connectivity MRI. *Cereb Cortex*. 2018;28:3095–114.
58. Lake EM, Finn ES, Noble SM, Vanderwal T, Shen X, Rosenberg MD, et al. The functional brain organization of an individual allows prediction of measures of social abilities transdiagnostically in autism and attention-deficit/hyperactivity disorder. *Biol Psychiatry*. 2019;86:315–26.
59. Markello RD, Hansen JY, Liu Z-Q, Bazinet V, Shafiei G, Suárez LE, et al. neuromaps: structural and functional interpretation of brain maps. *Nat Methods*. 2022;19:1472–9.
60. Hansen JY, Shafiei G, Markello RD, Smart K, Cox SML, Nørgaard M, et al. Mapping neurotransmitter systems to the structural and functional organization of the human neocortex. *Nat Neurosci*. 2022. <https://doi.org/10.1038/s41593-022-01186-3>.
61. Yamashita M, Kawato M, Imamizu H. Predicting learning plateau of working memory from whole-brain intrinsic network connectivity patterns. *Sci Rep*. 2015;5:7622.
62. Scheinost D, Noble S, Horien C, Greene AS, Lake EM, Salehi M, et al. Ten simple rules for predictive modeling of individual differences in neuroimaging. *Neuroimage*. 2019;193:35–45.
63. Kazeminejad A, Sotero RC. Topological properties of resting-state fMRI functional networks improve machine learning-based autism classification. *Front Neurosci*. 2018;12:1018.
64. Lanka P, Rangaprakash D, Dretsch MN, Katz JS, Denney TS Jr, Deshpande G. Supervised machine learning for diagnostic classification from large-scale neuroimaging datasets. *Brain Imaging Behav*. 2020;14:2378–416.
65. Padmanabhan A, Lynn A, Foran W, Luna B, O’Hearn K. Age related changes in striatal resting state functional connectivity in autism. *Front Hum Neurosci*. 2013;7:814.
66. Cerliani L, Mennes M, Thomas RM, Di Martino A, Thioux M, Keyers C. Increased functional connectivity between subcortical and cortical resting-state networks in autism spectrum disorder. *JAMA Psychiatry*. 2015;72:767–77.
67. Park S, Haak KV, Cho HB, Valk SL, Bethlehem RAI, Milham MP, et al. Atypical integration of sensory-to-transmodal functional systems mediates symptom severity in autism. *Front Psychiatry*. 2021;12:699813.
68. Hong S-J, Vos de Wael R, Bethlehem RAI, Larivière S, Paquola C, Valk SL, et al. Atypical functional connectome hierarchy in autism. *Nat Commun*. 2019;10:1022.
69. Yerys BE, Gordon EM, Abrams DN, Satterthwaite TD, Weinblatt R, Jankowski KF, et al. Default mode network segregation and social deficits in autism spectrum disorder: Evidence from non-medicated children. *Neuroimage Clin*. 2015;9:223–32.
70. Muller CL, Anacker AMJ, Veenstra-VanderWeele J. The serotonin system in autism spectrum disorder: from biomarker to animal models. *Neuroscience*. 2016;321:24–41.
71. Hamilton PJ, Campbell NG, Sharma S, Erreger K, Herborg Hansen F, Saunders C, et al. De novo mutation in the dopamine transporter gene associates dopamine dysfunction with autism spectrum disorder. *Mol Psychiatry*. 2013;18:1315–23.
72. Kaneko A, Ohshima R, Noda H, Matsumaru T, Iwanaga R, Ide M. Sensory and social subtypes of Japanese individuals with autism spectrum disorders. 2023;53:3133–43.
73. Thyé MD, Bednarz HM, Herringshaw AJ, Sartin EB, Kana RK. The impact of atypical sensory processing on social impairments in autism spectrum disorder. *Dev Cogn Neurosci*. 2018;29:151–67.
74. Cross-Disorder Group of the Psychiatric Genomics Consortium. Identification of risk loci with shared effects on five major psychiatric disorders: a genome-wide analysis. *Lancet*. 2013;381:1371–9.
75. Chen H, Uddin LQ, Duan X, Zheng J, Long Z, Zhang Y, et al. Shared atypical default mode and salience network functional connectivity between autism and schizophrenia. *Autism Res*. 2017;10:1776–86.
76. Oliver LD, Moxon-Emre I, Lai M-C, Grennan L, Voineskos AN, Ameis SH. Social cognitive performance in schizophrenia spectrum disorders compared with autism spectrum disorder: a systematic review, meta-analysis, and meta-regression. *JAMA Psychiatry*. 2021;78:281–92.
77. Jutla A, Foss-Feig J, Veenstra-VanderWeele J. Autism spectrum disorder and schizophrenia: an updated conceptual review. *Autism Res*. 2022;15:384–412.
78. Hong S-J, Valk SL, Di Martino A, Milham MP, Bernhardt BC. Multidimensional neuroanatomical subtyping of autism spectrum disorder. *Cereb Cortex*. 2018;28:3578–88.
79. Urchs SGW, Tam A, Orban P, Moreau C, Benhajali Y, Nguyen HD, et al. Functional connectivity subtypes associate robustly with ASD diagnosis. *Elife*. 2022;11:e56257.
80. Tang S, Sun N, Floris DL, Zhang X, Di Martino A, Yeo BTT. Reconciling dimensional and categorical models of autism heterogeneity: a brain connectomics and behavioral study. *Biol Psychiatry*. 2020;87:1071–82.
81. Tung Y-H, Lin H-Y, Chen C-L, Shang C-Y, Yang L-Y, Hsu Y-C, et al. Whole brain white matter tract deviation and idiosyncrasy from normative development in autism and ADHD and unaffected siblings link with dimensions of psychopathology and cognition. *Am J Psychiatry*. 2021;178:730–43.
82. Benkarim O, Paquola C, Park B-Y, Hong S-J, Royer J, Vos de Wael R, et al. Connectivity alterations in autism reflect functional idiosyncrasy. *Communications Biology*. 2021;4:1–15.
83. Hahamy A, Behrmann M, Malach R. The idiosyncratic brain: distortion of spontaneous connectivity patterns in autism spectrum disorder. *Nat Neurosci*. 2015;18:302–9.
84. Dinga R, Schmaal L, Penninx BWJH, van Tol MJ, Veltman DJ, van Velzen L, et al. Evaluating the evidence for biotypes of depression: methodological replication and extension of. *Neuroimage Clin*. 2019;22:101796.
85. Yamada T, Hashimoto R-I, Yahata N, Ichikawa N, Yoshihara Y, Okamoto Y, et al. Resting-state functional connectivity-based biomarkers and functional MRI-based neurofeedback for psychiatric disorders: a challenge for developing therapeutic biomarkers. *Int J Neuropsychopharmacol*. 2017;20:769–81.
86. Christensen DL, Braun KVN, Baio J, Bilder D, Charles J, Constantino JN, et al. Prevalence and characteristics of autism spectrum disorder among children aged 8 years - autism and developmental disabilities monitoring network, 11 sites, United States, 2012. *MMWR Surveill Summ*. 2018;65:1–23.
87. Reiter MA, Mash LE, Linke AC, Fong CH, Fishman I, Müller R-A. Distinct patterns of atypical functional connectivity in lower-functioning autism. *Biol Psychiatry Cogn Neurosci Neuroimaging*. 2019;4:251–9.
88. Whelan R, Garavan H. When optimism hurts: inflated predictions in psychiatric neuroimaging. *Biol Psychiatry*. 2014;75:746–8.

ACKNOWLEDGEMENTS

We are very grateful to the participants in the SRPBS, ABIDE-I, ABIDE-II, HBN, and BMB projects. This study was supported by AMED under Grant Number JP18dm0307008 and JP24wm0625502. Furthermore, this study was partly supported by JSPS KAKENHI under Grant Numbers JP21H05171, JP21H05174 and JP23H04979; AMED under Grant Numbers JP19dm0307105, JP19dm0207069, JP18dm0307001, JP18dm0307004, JP18dm0307009, and JP23wm0625001; Moonshot R&D under Grant Number JPMJMS2021; UTokyo Institute for Diversity and Adaptation of Human Mind (UTIDAHM); and the International Research Center for Neurointelligence (WPI-IRCN) at The University of Tokyo Institutes for Advanced Study (UTIAS). ABIDE-I was supported by NIMH (K23MH087770), NIMH (R03MH096321), Leon Levy Foundation, Joseph P. Healy, and the Stavros Niarchos Foundation. ABIDE-II was supported by NIMH (5R21MH107045), NIMH (5R21MH107045), Nathan S. Kline Institute of Psychiatric Research, Joseph P. Healey, Phyllis Green, and Randolph Cowen.

AUTHOR CONTRIBUTIONS

TI, AY, MK, and RH designed the study. TI, NY, JF, YY, MN, RA, YYA, TO, HO, MT, NI, GO, NO, KK, YO, NK, and HT recruited the participants of the study and collected the

clinical and imaging data. TI and AY analyzed of the data. TI, AY, and RH wrote the original draft of the manuscript. TI, AY, YT, NY, YYA, JF, YY, MN, RA, TO, HO, YS, MT, NI, GO, NO, KK, SCT, HI, NK, YO, HT, MK, OY, and RH reviewed and revised the manuscript.

COMPETING INTERESTS

MK is an inventor of patents owned by the Advanced Telecommunications Research Institute International related to the present work (PCT/JP2014/061544 [WO2014178323] and JP2015-228970/6195329). AY and MK are inventors of a patent application submitted by the Advanced Telecommunications Research Institute International related to the present work (JP2018-192842). YT is an employee of SHIONOGI & CO., LTD. YS and MK are employees of XNef Inc.

ADDITIONAL INFORMATION

Supplementary information The online version contains supplementary material available at <https://doi.org/10.1038/s41380-024-02759-3>.

Correspondence and requests for materials should be addressed to Ryu-ichiro Hashimoto.

Reprints and permission information is available at <http://www.nature.com/reprints>

Publisher's note Springer Nature remains neutral with regard to jurisdictional claims in published maps and institutional affiliations.



Open Access This article is licensed under a Creative Commons Attribution-NonCommercial-NoDerivatives 4.0 International License, which permits any non-commercial use, sharing, distribution and reproduction in any medium or format, as long as you give appropriate credit to the original author(s) and the source, provide a link to the Creative Commons licence, and indicate if you modified the licensed material. You do not have permission under this licence to share adapted material derived from this article or parts of it. The images or other third party material in this article are included in the article's Creative Commons licence, unless indicated otherwise in a credit line to the material. If material is not included in the article's Creative Commons licence and your intended use is not permitted by statutory regulation or exceeds the permitted use, you will need to obtain permission directly from the copyright holder. To view a copy of this licence, visit <http://creativecommons.org/licenses/by-nc-nd/4.0/>.

© The Author(s) 2024